Scripta Materialia 145 (2018) 113–117

Contents lists available at ScienceDirect

Scripta Materialia

journal homepage: www.elsevier.com/locate/scriptamat

Regular article

Columnar to equiaxed transition in Al-Mg(-Sc)-Zr alloys produced by selective laser melting

Kun V. Yang [a,b,c,*], Yunjia Shi [a,d], Frank Palm [e], Xinhua Wu [a,b], Paul Rometsch [a,b]

[a] Department of Materials Science and Engineering, Monash University, Melbourne, VIC 3800, Australia
[b] Monash Centre for Additive Manufacturing, 13 Normanby Road, Notting Hill, VIC 3168, Australia
[c] CSIRO Manufacturing, Clayton, VIC 3168, Australia
[d] School of Physics and Engineering, Zhengzhou University, Zhengzhou 450052, PR China
[e] Airbus, Airbus Central Research & Technology (CRT), Department XRS, Ottobrunn, Germany

ARTICLE INFO

Article history:
Received 13 June 2017
Received in revised form 27 September 2017
Accepted 17 October 2017
Available online xxxx

Keywords:
Selective laser melting
Columnar to equiaxed transition
Aluminium scandium alloys
Thermal gradients
Grain refinement

ABSTRACT

The addition of 1.08 wt% Sc to an Al-Mg-Zr alloy produced by selective laser melting modifies the highly coarse columnar grain structure to significantly refined columnar grains separated by sub-micron equiaxed grains at the melt pool boundaries. The latter nucleate mainly from the Al_3Sc particles in the remelting zone. An almost fully equiaxed grain structure was achieved by increasing the applied volumetric energy density from 77.1 J/mm^3 to 154.2 J/mm^3 and the platform temperature from 35 °C to 200 °C, due to the combined effects of potent nuclei, increased remelting zone volumes and reduced thermal gradients.

Metal selective laser melting (SLM) processes are poised to transform the metal manufacturing industry, particularly in those areas where conventional manufacturing reaches its limitations in terms of both design freedom and manufacturing capabilities [1]. However, one of the key technical problems of the current light metal alloys for SLM, including Al alloys, is that the majority of them suffer from significant anisotropy in properties such as yield strength and elongation to fracture (e.g. SLM-processed Al-7Si-Mg alloy [2]), which increases the difficulty and reduces the freedom of the component design. This is a direct result of the highly columnar grains with major epitaxial grain growth through melt pool boundaries along the building direction [3–5], due to the generation of very high thermal gradients and cooling rates that are orders of magnitude higher than for conventional casting processes. Scalmalloy®, a Sc- and Zr-modified 5xxx alloy developed by the Airbus Group, is one exception. The SLM-processed Scalmalloy® has shown regimes with sub-micron grain sizes mainly at the melt pool boundaries, and indeed an anisotropy in yield strength of <4% is obtained for the as-fabricated material [6]. However, around 50–80% of the microstructure is still dominated by columnar grains although these columnar grains are 5–10 times shorter than in other SLM-processed aluminium alloys [6]. The current work aims to better understand the formation mechanism of these two distinct grain structures for a similar SLM-processed Al-Mg-Sc-Zr alloy, and to demonstrate how the microstructure can be tuned in terms of the volume fraction ratio of columnar to equiaxed grains. A similar Al-Mg-Zr alloy but without Sc was also investigated for comparison.

The chemical compositions of the pre-alloyed powders used for SLM are shown in Table 1. Samples were manufactured on an EOSINT M280 powder bed machine with a laser beam diameter of 100 μm, laser power of 370 W (P), hatch distance of 0.10 mm (h), layer thickness of 0.03 mm (t), and laser scanning speed (v) of 800 mm/s and 1600 mm/s. Cubes measuring 18 mm × 18 mm × 10 mm were deposited onto Al substrates heated to 35 °C or 200 °C, using a bi-directional scan strategy. The samples with different processing parameters were labelled A, B, C, and D, respectively (Table 2). Applied volumetric energy density, defined by $E = P/vht$, was used to evaluate the energy input. Samples were cut along the building direction, and polished using standard metallographic methods down to 0.05 μm colloidal silica for Electron Backscatter Diffraction (EBSD) observation using a FEI Quanta 3D FEG FIB scanning electron microscope. For the Al-Mg-Zr alloy, an area of 625 μm by 625

Table 1
Chemical compositions of the alloys investigated.

Element (wt%)	Mg	Sc	Mn	Cu	Zr	Si	Fe	Al
Al-Mg-Sc-Zr	3.40	1.08	0.50	0.44	0.23	0.14	0.08	Bal.
Al-Mg-Zr	4.15	–	0.39	–	0.21	0.17	0.13	Bal.

* Corresponding author.
E-mail address: kun.yang@monash.edu (K.V. Yang).

https://doi.org/10.1016/j.scriptamat.2017.10.021
1359-6462/

Table 2
Processing parameters for different samples investigated.

Al-Mg-Zr and Al-Mg-Sc-Zr alloys							Al-Mg-Sc-Zr alloy	
Sample	Laser power (W)	Scanning speed (mm/s)	Hatch distance (mm)	Layer thickness (mm)	Platform temperature (°C)	$E = P/vht$ (J/mm^3)	Volume fraction of equiaxed grains (%)	Equiaxed grain diameter (μm)
A	370	1600	0.1	0.03	35	77.1	64.2	0.8
B	370	800	0.1	0.03	35	154.2	65.6	0.9
C	370	1600	0.1	0.03	200	77.1	71.3	0.8
D	370	800	0.1	0.03	200	154.2	100	1.5

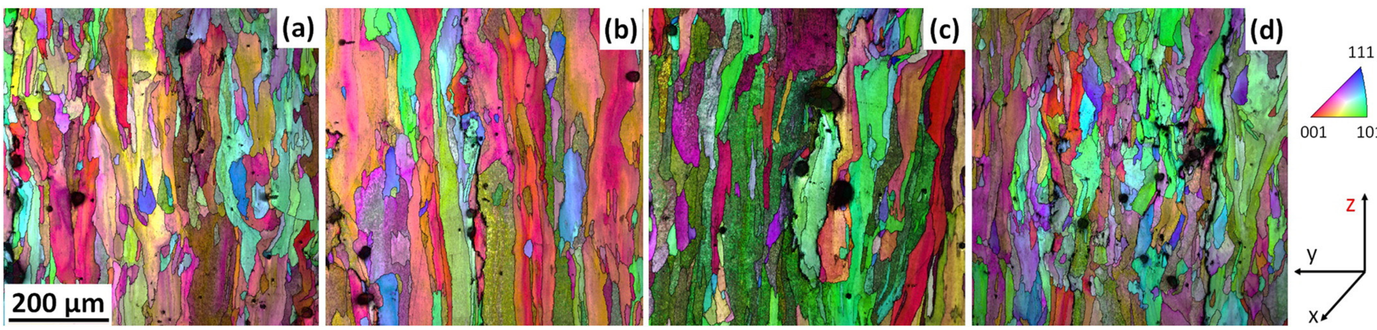

Fig. 1. Microstructures reconstructed from inverse pole figures obtained from EBSD measurement on the Al-Mg-Zr alloy. (a) E = 77.1 J/mm^3, platform temperature of 35 °C; (b) E = 154.2 J/mm^3, platform temperature of 35 °C; (c) E = 77.1 J/mm^3, platform temperature of 200 °C; (d) E = 154.2 J/mm^3, platform temperature of 200 °C.

μm with a step size of 2 μm was scanned using EBSD. The scanned area for the low magnification EBSD map for the Al-Mg-Sc-Zr alloy was 200 μm by 200 μm with a step size of 0.2 μm, and 50 μm by 50 μm with a step size of 0.05 μm for the high magnification.

Microstructures reconstructed from inverse pole figures obtained by EBSD measurements of the Al-Mg-Zr alloy are shown in Fig. 1. Intergranular cracks and round defects ranging from 5 to 50 μm are found for this alloy (dark lines and circles). Not surprisingly, large columnar grains[1] along the building direction (z) around 600 μm in length are observed as a result of high thermal gradients in the melt pool. It should be noted that because a layer thickness of 30 μm was used, the large columnar grains in the Al-Mg-Zr alloy therefore must have been formed by epitaxial grain growth through melt pool boundaries. It should also be noted that in the current paper, the melt pool is defined as the region with liquid fraction ranging from 0 to 1, which includes the partially melted/liquated zone formed by remelting the previous layer. As for samples with different processing conditions, no significant differences were found, except for sample D, which shows an increased portion of grains with smaller aspect ratio and a decreased pore size.

By contrast, the Al-Mg-Sc-Zr alloy shows no large defects in the scanned area and a significantly refined grain microstructure, which can essentially be divided into two regimes (Fig. 2): (i) superfine equiaxed grains at the melt pool boundaries, and (ii) either columnar grains or relatively larger equiaxed grains at the top of melt pools. Compared with the Al-Mg-Zr alloy, the columnar grains found in the Al-Mg-Sc-Zr alloy are at least an order of magnitude finer (around 20 μm to 60 μm in length), and the equiaxed grains are around 1 μm or less in diameter. Similar grain microstructures have been found previously for an SLM-processed Al-Sc based alloy [6]. The fine-grained regime was also found at the melt pool base in a narrow band where temperatures rose up to around 800 °C (above which Al_3Sc phases re-dissolve) during laser re-melting of the previous layer [6]. Although it was claimed that both Al_3Sc particles and Mg-containing oxides were associated with the fine-grained regime [6], the formation mechanism of these superfine equiaxed grains is still unclear.

In the current work, we propose that it is the Al_3Sc particles that are primarily responsible for the equiaxed grain formation by heterogeneous nucleation. Equiaxed grain formation, is normally promoted by a low thermal gradient (G) to growth rate (R) ratio [7]. In conventional casting, the solidification normally starts at a mould wall where G is highest and then progresses towards lower G regions where equiaxed grains may form, though a chill zone with equiaxed grains may also occur at the mould wall [7,8]. In fusion welding, G is highest at the fusion line where solidification starts (low R), and lowest at the last-to-solidify trailing edge, or centre line, where R reaches its maximum [9–11]. This is why equiaxed grains may form unaided at the centre line in fusion welding [10]. However, when applying the thermal gradient distribution pattern in fusion welding to SLM, the magnitude of G is normally still too high to generate unaided equiaxed grain formation even towards the top of a melt pool despite the higher thermal undercooling in SLM. Simulations have shown that in SLM, thermal gradients of the order of 10^6–10^7 K/m are reached [12], which is six orders of magnitude higher than typical thermal gradients in sand castings (~1 K/m, [13]). This can lead to extremely large G/R values and hence cellular microstructure and columnar grain formation in SLM [14], as observed for most SLM-processed alloys [2,4,15–18], including the Al-Mg-Zr alloy in the current study. Having said that, all the discussions above have not considered the presence of a high density of nucleation sites (N_0) in the melt, which indeed plays a critical role in equiaxed grain formation [9–11]. Especially when a high thermal gradient is present, the number of nucleation sites is of more importance according to Hunt criterion [19]. Therefore, we propose that the superfine bands of equiaxed grains in Fig. 2 and references [6,20] are primarily a result of the remnant of a large amount of Al_3Sc nucleants in the semi-solid/liquated zone at the bottom of the melt pool due to remelting of the previous layer. By providing a high density of low-energy-barrier heterogeneous nucleation sites ahead of the solidification front, the critical amount of total undercooling needed to induce equiaxed grain growth is reduced.

[1] In this study, the aspect ratio for columnar grains is defined as larger than 3:1 in terms of the length to width ratio, whereas the aspect ratio for equiaxed grains is defined as equal to or smaller than 3:1.